Physica Medica 30 (2014) 854–857

Contents lists available at ScienceDirect

Physica Medica

journal homepage: http://www.physicamedica.com

Technical notes

Measuring output factors and beam profiles formed by multileaf collimators using Fricke gel dosimeter

Lucas Nonato de Oliveira [a,b,*], Adelaide de Almeida [c], Linda V.E. Caldas [b]

[a] Instituto Federal de Educação, Ciência e Tecnologia de Goiás (IFG), Inhumas, GO, Brazil
[b] Instituto de Pesquisas Energéticas e Nucleares (IPEN/CNEN), São Paulo, SP, Brazil
[c] Departamento de Física, FFCLRP – Universidade de São Paulo (USP), Ribeirão Preto, SP, Brazil

ARTICLE INFO

Article history:
Received 4 December 2013
Received in revised form
12 March 2014
Accepted 1 April 2014
Available online 24 April 2014

Keywords:
Fricke xylenol gel
Multileaf collimator
Small fields

ABSTRACT

The accuracy and precision are necessary factors in radiotherapy, especially for measurements involving output factors and beam profiles; in this case multileaf collimators (MLCs) and dosimeter systems are not employed to obtain an adequate absorbed dose. In this work, output factors and beam profiles using multileaf collimators were obtained through the Fricke Xylenol Gel (FXG) dosimeter irradiated with 6 MV photon beams. From the results, FXG dosimetry demonstrated to be an adequate dosimetric tool for radiotherapy applications using MLC.

Introduction

In radiotherapy, the radiation from a linear accelerator with beams of photons and/or electrons is used to neutralize or kill cancerous cells. Subsequently, these beams are collimated to avoid scatterings that may occur and compromise the absorbed dose prescribed by the radiotherapist [1–3]. New technologies are being developed for a better absorbed dose delivery to the patient, ensuring a precision better than 5% [4]. A tool for the accuracy and precision of the equipment dose delivery is the multileaf collimator (MLC) system; it consists of a series of computer-controlled tungsten leaf pairs that can independently slide in and out of the radiation beam, thus adjusting the size and shape of the beam field [5]. The MLC system has advantages such as replacing conventional blocks, it can be applied in beam's eye view (BEV), projection of the planning target volume (RTV) and beam-intensity modulation (IMRT), due to the scattering in the multileaf system and the knowledge of the beam format on the target are respectively necessary measurements of the output factors and profiles of the beams for the planning system, at the time of absorbed dose delivery to the patient [6,7]. Finally, the dosimetric system with high resolution measurements should be used with MLC, for a 3D dosimetry of the entire treatment [8–10].

The Fricke Xylenol Gel (FXG) dosimeter is promising for the MLC dosimetry, once it can be specific for photon and electron beams small fields dosimetry [11–14], and it has characteristics suitable for use in the measurements required in MLC. This irradiated dosimeter oxidizes Fe^{+2} to Fe^{+3} ions, which is proportional to the absorbed dose. Features such as effective atomic number and density, near the soft tissues, make this phantom-dosimeter applicable for radiotherapy and researches using the FXG with low and high photons and electrons energies can be found in the literature [15–17].

Output factors and beam profiles are physical characteristics also useful with multileaf collimators in clinical radiotherapy. In this work, the application of the FXG dosimeter can be useful due to the utilization of irradiationa phantom in 3D [18].

The main purpose of this work was to determine the output factors and beam profiles for photon small fields, through MLC, using the FXG dosimeter.

Material and methods

The Fricke Xylenol Gel (FXG) dosimeter used is composed of: gelatin 300 Bloom, sulfuric acid, ferrous sulfate, xylenol orange and Milli-Q water. Its preparation [19–21], irradiation [22,23] and applications [24–26] were already reported [27–32]. The FXG optical density was determined from a portable spectrometer (Vary-

* Corresponding author. Instituto Federal de Educação, Ciência e Tecnologia de Goiás (IFG), Inhumas, GO, Brazil. Tel./fax: +55 62 3514 9500.
E-mail addresses: lucas@ifg.edu.br, lucasifg@yahoo.com.br (L. Nonato de Oliveira).

http://dx.doi.org/10.1016/j.ejmp.2014.04.001
1120-1797/

Varian/Ultro-pec2100/79500), with the wavelength at 585 nm and a light collimator of 1 mm diameter, that determines the FXG lateral spatial resolution.

The protocol of the FXG dosimeter preparation [19–21] considers that for a desired dosimeter volume, 75% of it is composed of Milli-Q water, highly purified. This preparation, for example, requires that for a dosimeter of 1000 ml of water, 750 ml of it be mixed with 50.058 g of pig skin gelatin (Sigma–Aldrich 300 Bloom) for a time of 15 min and temperature of 45 °C, in order to obtain a clear and homogeneous solution. Thereafter, no more than 30 min, 12.5% of the remaining 25% water has to be mixed with 2.386 g of sulfuric acid + 0.076 g of Xylenol Orange and added to the previous solution, stirring for better homogenization, followed by the addition of 0.196 g of Ferrous Sulphate mixed with the remaining 12.5% of water, stirring again to obtain the final solution that has to be refrigerate at 10 °C for 30 min. From measurements for this dosimeter [11,12,23], the absorbed dose response for 6 MV photon beam is linear in the range 0.1–30.0 Gy, with a sensitivity (slope of the dose response) around 0.08 Gy^{-1} [11]. The reproducibility and stability were possible within 5 h post irradiation [23] keeping the cuvettes refrigerated between measurements.

The Beam profile (BP) and Output factor (OF), were obtained from 6 MV photon beams, from a Varian 2100C linear accelerator with 26 pairs multileaf collimators. The measurements were done with a source to surface distance of 100 cm, at maximum depth of d_{max} = 1.5 cm and with an absorbed dose of 3 Gy. The small field sizes: 1 × 1, 2 × 2, 3 × 3 and 4 × 4 cm^2 were shaped with the multileaf collimators; and during the measurements the jaws collimators were set to a field of 10 × 10 cm^2. The experimental set-up is shown in Fig. 1, with the FXG cuvettes (1 × 1 × 10 cm^3) immersed in an acrylic-water phantom (30 × 30 × 40 cm^3). The FXG absorbance readings, proportional to the absorbed dose in the dosimeter, were inferred from the transmission measurements and were normalized to the maximum absorbed dose value in the beam central axis.

The beam profiles were obtained using the FXG with readings along the dimension of 10 cm of the cuvettes, through Eq. (1):

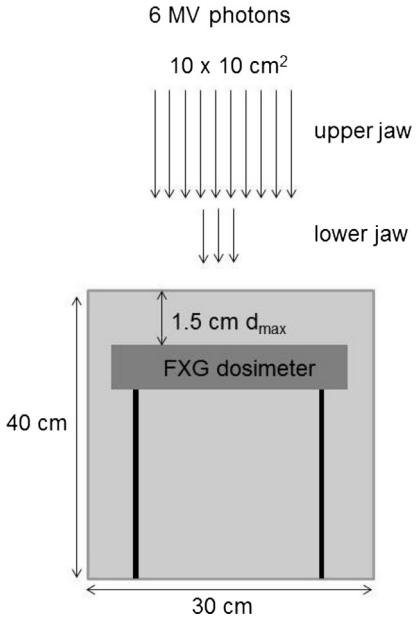

Figure 1. Experimental set-up showing the primary collimator jaws which remained fixed at 10 × 10 cm^2 (upper) and secondary collimators (lower) which formed small fields less than 4 × 4 cm^2. The FXG sample was inserted in the water phantom at a maximum distance of 1.5 cm and irradiated with 6 MV photons.

$$BP = \frac{D_i}{D_c} \quad (1)$$

where D_i and D_c are, respectively, the absorbed dose values along the field and at the buildup position in the central axis.

The output factors were obtained from the FXG readings at the center of cuvettes for different field sizes, related to that acquired for the reference field size (10 × 10 cm^2) through Eq. (2):

$$OF = \frac{D_f}{D_{10}} \quad (2)$$

D_f and D_{10} are respectively, the absorbed dose value for a selected field size and for the reference field size.

The small field sizes beam penumbras were determined at the maximum distance and were characterized in the space interval in which the absorbed dose rises from 20% to 80% of the central absorbed dose, increasing with the increase of the scatter added into the beam line due to the increase of the irradiated volume [5].

For measurements with dosimeter gels, when the diffusion has to be considered, their diffusion coefficients should be used to correct the results according to the post-irradiation time [33–37]. In this study, the diffusion coefficient was not used for the absorbance measurements, once they were taken immediately after irradiation (in average 2 min, with a fading of 0.04%). If a diffusion coefficient correction was needed, this could be done by the methods described in the literature [38], measurements that consider the same FXG dosimeter solution presented in this work.

Results and discussion

Small field profiles obtained from MLC are shown in Fig. 2. If can be seen that smaller the field it goes from a square shape profile to a quasi Gaussian one [10]. The profile gradients, situated between 80% and 20% of the dose absorbed, are the interval or region where the penumbra is obtained [39].

In Fig. 3, the penumbra width ranged linearly from 2.0 mm to 7.0 mm for the 6 MV photon beams; these values are in agreement with the values derived from other methods such as point spread and line spread function analyses [40].

Output factor values are shown in Fig. 4, initially with a lower value, increasing faster, for smaller fields sizes, and tending to a constant value, with the increase of the field size up to the reference one of 10 × 10 cm^2. The higher the volume irradiated, more difficult

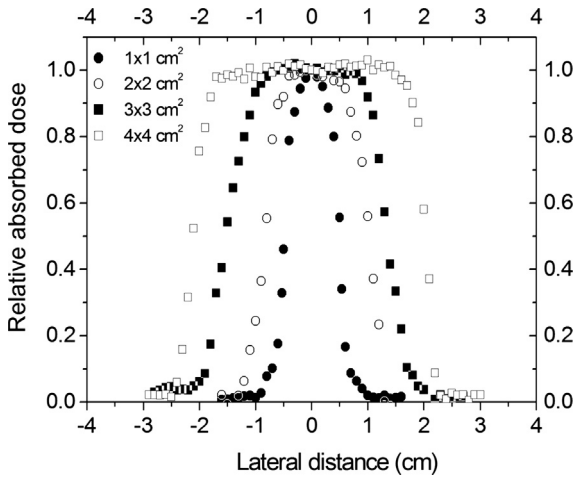

Figure 2. FXG beam profiles for 6 MV photon beams using square field sizes of 1 × 1, 2 × 2, 3 × 3 and 4 × 4 cm^2 formed by MLC.

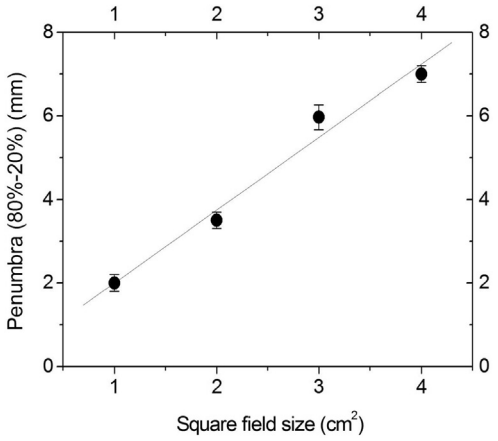

Figure 3. MLC penumbra widths 80%–20% *versus* field size for 6 MV photon beams calculated through the experimental data of beam profiles measured with FXG.

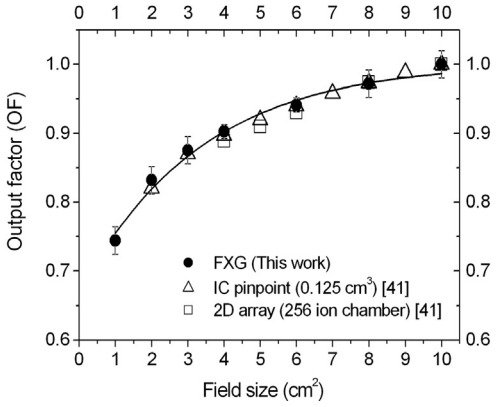

Figure 4. 6 MV photon output factor for FXG dosimeter using MLC, with small field sizes of 1 × 1, 2 × 2, 3 × 3, 4 × 4, 6 × 6, 8 × 8 and 10 × 10 cm^2.

it is for the field scatter to approach the center, when comparing with smaller volumes (smaller field sizes). These results are consistent with output factors determined using other types of dosimeters such as: ionization chamber (PTW, Freiburg, Germany, 0.125 cm^3) and 2D Array Seven29™ (PTW, Freiburg, Germany, 256 ion chamber array, 0.125 cm^3) [41].

Conclusions

From the results, it can be concluded that: 1) The beam profiles for small fields were determined in agreement with the high resolution of the FXG dosimetric system; 2) The accuracy and precision importance in the output factor determination was verified, to be accounted for the decision related to the absorbed dose delivery to the patient and 3) The penumbra obtained at a maximum of 7 mm is within the established maximum tolerance of 13 mm [5,14]. This work shows that the FXG dosimeter can as well be applied for the determination of dosimetric characteristics (output factors and beam profiles) of MLC small field sizes.

Acknowledgments

This research was supported by CNPq (Conselho Nacional de Desenvolvimento Científico e Tecnológico) grant numbers (150774/2012-5 and 304789/2011-9) and FAPEG (Fundação de Amparo a Pesquisa do Estado de Goiás) grant number (201200555780002). The authors are grateful to the Radiotherapy Department of the Hospital Araújo Jorge, Goiânia, Goiás.

References

[1] IAEA. Commissioning and quality assurance of computerized planning systems for radiation treatment of cancer. Technical Reports series No. 430; 2004.
[2] Johns HE, Cunningham JR. The physics of radiology. American Lecture. 4th ed. Ilinois: Charles Thomas, Springfield; 1983. p. 796.
[3] Khan FM. The physics of radiation therapy. 3rd ed. Philadelphia: Lippincott Lippincott Williams & Wilkins; 1993.
[4] Brahme A. Dosimetric precision requirements in radiation therapy. Acta Radiol Oncol 1984;23:379–91.
[5] AAPM. Basic applications of multileaf collimators. Report No. 72; 2001.
[6] Alaei P, Higgins P. Effect of multileaf collimator-defined segment size on S(c). Med Phys 2010;37:2731–7.
[7] Stathakis S, Esquivel C, Gutiérrez AN, Shi C, Papanikolaou N. Dosimetric evaluation of multi-pattern spatially fractionated radiation therapy using a multi-leaf collimator and collapsed cone convolution superposition dose calculation algorithm. Appl Radiat Isot 2009;67:1939–44.
[8] Killoran JH, Giraud JY, Chin L. A dosimetric comparison of two multileaf collimator designs. Med Phys 2002;29:1752–8.
[9] Loi G, Pignoli E, Scorsetti M. Design and characterization of a dynamic multileaf collimator. Phys Med Biol 1998;43:3149–55.
[10] Meeks SL, Bova FJ, Kim S, Tome WA, Buatti JM. Dosimetric characteristics of a double-focused miniature multileaf collimator. Med Phys 1999;26:729–33.
[11] Calcina CSG, Oliveira LN, Almeida CE, Almeida A. Dosimetric parameters for small field sizes using Fricke xylenol gel, thermoluminescent, film dosimeters,and an ionization chamber. Phys Med Biol 2007;52:1431–9.
[12] Oliveira LN, Calcina CSG, Parada MA, Almeida CE, Almeida A. Ferrous xylenol gel measurements for 6 and 10 MV Photons in small field sizes. Braz J Phys 2007;27:1141–6.
[13] Pirani LF, Moreira MV, Costa JJL, Oliveira LN, Caldas LVE, Almeida A. Fricke dosimeter gel measurements of the profiles of shielded fields. Appl Radiat Isot 2013;82:239–41.
[14] Sampaio FGA, Oliveira LN, Moreira MV, Petchevist PCD, Almeida CE, Almeida A. 8 and 10 MeV Electron beams small field-size dosimetric parameters through the fricke xylenol gel dosimeter. IEEE Trans Nucl Sci 2013a;60:572–7.
[15] Bartesaghi G, Burian J, Gambarini G, Marek M, Negri A, Viererbl L. Evaluation of all dose components in the LVR-15 reactor epithermal neutron beam using Fricke gel dosimeter layers. Appl Radiat Isot 2009;67:S199–201.
[16] Carrara M, Fallai C, Gambarini G, Negri A. Fricke gel-layer dosimetry in high dose-rate brachytherapy. Appl Radiat Isot 2010;68:722–5.
[17] Pirani LF, Oliveira LN, Petchevist PCD, Moreira MV, Ila D, Almeida A. New chemical Fricke gel radiation dosimeter. J Radioanal Nucl Chem 2009;280:259–62.
[18] Sampaio FGA, Del Lama LS, Sato R, de Oliveira DMM, Czelusniak C, Oliveira LN, et al. Quality assurance of a two-dimensional CCD detector system applied in dosimetry. IEEE Trans Nucl Sci 2013b;60:810–6.
[19] Bero MA, Gilboy WB, Glover PM, Keddie JL. Three-dimensional radiation dose measurements with Ferrous Benzoic Acid Xylenol Orange in Gelatin gel and optical absorption tomography. Nucl Instr Meth Phys B 1999;422:617–20.
[20] Bero MA, Gilboy WB, Glover PM, El-Masri HM. Tissue-equivalent gel for non-invasive spatial radiation dose measurements. Nucl Instr Meth Phys B 2000;166:820–5.
[21] Bero MA, Gilboy WB, Glover PM. Radiochromic gel dosemeter for three-dimensional dosimetry. Radiat Phys Chem 2001;61:433–5.
[22] Oliveira LN, Zimmerman RL, Moreira MV, Ila D, Almeida A. Determination of diffusion coefficient in Fricke Xylenol gel dosimeter after electron beam bombardment. Surf Coat Tech 2009;203:2367–9.
[23] Oliveira LN, Calcina CSG, Parada MA, Almeida CE, Almeida A. 6 MV Wedge photon beam profiles with the fricke xylenol gel dosimeter. Braz J Phys 2009;39:615–8.
[24] Abukassem I, Bero MA. Application of radiochromic gel detector (FXG) for UVA dose measurements. Radiat Phys Chem 2010;79:1209–14.
[25] Alva-Sánchez MS, Oliveira LN, Petchevist PC, Moreira MV, Almeida A. Beta planar source quality assurance with the Fricke xylenol gel dosimeter. Radiat Phys Chem 2014;96:56–9.
[26] Davies JB, Baldock C. Temperature dependence on the dose response of the Fricke–gelatin–xylenol orange gel dosimeter. Radiat Phys Chem 2010;79:660–2.
[27] Rabaeh KA, Moussa AA, Basfar AA, Msalam RI. Novel radio-chromic solution dosimeter for radiotherapy treatment planning. Phys Med 2013;29:374–8.
[28] Bansal AK, Semwal MK, Arora D, Sharma DN, Julka PK, Rath GK. A phantom study on bladder and rectum dose measurements in brachytherapy of cervix cancer using FBX aqueous chemical dosimeter. Phys Med 2013;29:368–73.
[29] Keall P, Baldock C. A theoretical study of the radiological properties and water equivalence of three types of gels used for radiation dosimetry. Austr Phys Eng Sci Med 1999;22:85–91.
[30] Schreiner LJ. Review of Fricke gel dosimeters. J Phys Conf Ser 2004;3:9–21.
[31] Olsson LE, Appleby A, Sommer I. A new dosimeter based on ferrous sulphate solution and agarose gel. Appl Radiat Isot 1991;42:1081–6.

[32] Gambarini G, Arrigoni S. Dose-response curve slope improvement and result reproducibility of ferrous sulphate-doped gels analysed by NMR imaging. Phys Med Biol 1994;39:703–17.
[33] Harris PJ, Piercy A, Baldock C. A method for determining the diffusion coefficient in Fe (II/III) radiation dosimetry gels using finite elements. Phys Med Biol 1996;41:1745–53.
[34] Baldock C, Harris PJ, Piercy AR, Healy B. Experimental determination of the diffusion coefficient in two-dimensions in ferrous sulphate gels using the finite element method. Austr Phys Eng Sci Med 2001;24:19–30.
[35] Baldock C, Harris PJ, Piercy AR, Patval S, Prior DN, Keevil SF, et al. Investigation of temperature dependence of diffusion in agar Fricke gel for MRI dosimetry. Proc ISMRM 1994;22:1103–5.
[36] Kron T, Metcalfe P, Pope JM. Investigation of the tissue equivalence of gels used for NMR dosimetry. Phys Med Biol 1993;38:139–50.
[37] Chu WC, Wang J. Exploring the concentration gradient dependency of the ferric ion diffusion effect in MRI-Fricke-infused gel dosimetry. Phys Med Biol 2001;45:L63–4.
[38] Oliveira LN, Almeida A, Caldas LVE. Fricke gel diffusion coefficient measurements for applications in radiotherapy level dosimetry. Radiat Phys Chem 2014;98:42–5.
[39] International Atomic Energy Agency (IAEA). Aspectos físicos de la garantía de calidad: Protocolo de control de calidad, TECDOC-1151, 2000.
[40] Day MJ, Lambert GD, Locks SM. The effect of secondary electron spread on the penumbra in high energy photon beam therapy. Br J Radiol 1990;63:278–85.
[41] Spezi E, Angelini AL, Romani F, Ferri A. Characterization of a 2D ion chamber array for the verification of radiotherapy treatments. Phys Med Biol 2005;50:3361–73.